논문 01-02-14

Multitexture Image Segmentation Using Amplitude Demodulation

진폭복조를 이용한 복합텍스쳐영상의 분할

Hyun-Soo Lee*
(李 賢 秀*)

Abstract

This paper proposes a 2-D texture segmentation algorithm which is in close analogy to amplitude demodulation in communication systems. First, we show that it is theoretically possible to segment a multitexture image using an ideal filter followed by an amplitude demodulation block. However, in practice, the Gabor filter is used instead of the ideal filter because it has many desirable properties and especially it gives optimum space-bandwidth product. Our algorithm recovers all the texture regions containing the sinusoid with frequency to which the Gabor filter is tuned. We have demonstrated the discriminating power of our method in using a synthetic multitexture image. It is clear mathematically and easy to implement. Our method can be a good alternative to avoid many problems encountered in classifying the feature vectors in feature-based texture segmentation approaches.

요 약

본 논문에서는 통신시스템에서의 진폭복조와 유사한 알고리듬을 이용한 2 차원 텍스처 영상분할에 관해 소개한다. 우선 이상적인 필터링 후에 진폭복조를 함으로써 복합텍스쳐영상을 분할 할 수 있음을 이론적으로 보였다. 그러나 실재의 경우, 이상적인 필터 대신, 여러 가지 이점이 있고 특히 최적의 공간-대역폭적의 특성을 갖고 있는 게이버 필터를 사용하였다. 우리의 알고리듬은 게이버 필터의 동조주파수와 동일한 주파수의 정현파를 갖고 있는 텍스처 영역을 모두 찾아준다. 합성된 복합텍스쳐영상을 이용하여 본 논문에서 제의한 방법의 분할능력을 보였다. 이 방법은 수학적으로 명백하고 또한 적용하기에 용이하다. 이 방법은 특성기반 텍스쳐 분할방법에서 특성벡터 분류시 야기되는 많은 문제를 피할 수 있는 좋은 대안이 될 수 있다.

Keywords : Computer Vision, Texture Segmentation, Gabor Filter, Amplitude Demodulation, Image Segmentation

I. Introduction

Texture can be used in many applications in image analysis such as the recognition of an object using the texture as a surface in- formation of the corresponding object, to get the 3-D depth information, the information about the shape and orientation in images, and also the image segmentation to find out the

* 明知大學校 電子情報通信工學部
接受日: 2001年 8月30日, 修正完了日: 2001年11月26日

* (School of Electronics, Information and communication Eng., Myongji Uni.)

boundaries between different objects in an image. The result of the segmentation is very important for the next higher level processing results to be meaningful.

For the past twenty years, there has been a lot of work on texture segmentation[6] and there is a particularly strong concentration in the development of feature-based approaches. Most of these approaches use small window to slide on the image. At every step of window translation, a feature vector is calculated for that part of the image enclosed by the window. These vectors are finally classified in the feature vector space to obtain the segmented image.

But this method of texture segmentation based on classification has many problems. First, the problems inherent to the classification method itself : the high dimensionality of the feature vector, the great number of feature vectors to be classified.

To decide which features have to be chosen is another problem. They have to be chosen in such a way that they can distinguish the different textures in an optimal way. Even if the best features are chosen, feature vectors obtained when the window includes many texture boundaries lead to misclassification because these vectors have the fused characteristics of all the regions in the window.

Also, the size of the window influences the segmentation result.

We propose a texture segmentation method based on amplitude demodulation. Our method needs neither the window nor the classification, thus avoids all the problems mentioned above.

We use a synthetic 2-D multitexture image to verify the mathematical results developed in this paper.

Our method is very simple and efficient. First, we assume that every texture is distinguishable because each texture has its own dominant spatial frequencies different from those of the other textures. This assumption and the conjecture given at the very beginning of the Section Ⅱ lead us to the texture segmentation method based on Gabor filtering and Amplitude Demodulation.

Table 1. Schematic multitexture image representation
표 1. 복합텍스쳐 영상의 도식적 표현

$\boldsymbol{R}_1$ $(A_{11}, A_{12}, \ldots, A_{1j_1})$ $(f^x_{11}, f^x_{12}, \ldots, f^x_{1j_1})$ $(f^y_{11}, f^y_{12}, \ldots, f^y_{1j_1})$ $(\theta_{11}, \theta_{12}, \ldots, \theta_{1j_1})$ C_1		
		$\boldsymbol{R}_{i_1}$ $(A_{i_1 1}, A_{i_1 2}, \ldots, A_{i_1 j_{i_1}})$ $(f^x_{i_1 1}, f^x_{i_1 2}, \ldots, f^x_{i_1 j_{i_1}})$ $(f^y_{i_1 1}, f^y_{i_1 2}, \ldots, f^y_{i_1 j_{i_1}})$ $(\theta_{i_1 1}, \theta_{i_1 2}, \ldots, \theta_{i_1 j_{i_1}})$ C_{i_1}

Ⅱ. Multitexture Image Model

We conjecture that multitexture image is an ensemble of different texture regions $\boldsymbol{R}_i$ (i=1,...,i1), each of which can be represented again as an ensemble of many sinusoids and the mean value of the region, as given schematically in Table 1.

All the parameters in this table are,

A's : amplitudes of the sinusoids

f's : frequencies of the sinusoids

Θ's : phases of the sinusoids

C's : mean value of each texture region

Note that each texture region they can take any arbitrary form.

This conjecture gives rise to the multitexture image model $m(x,y)$ (see(1)), which is very important because all the results in this paper originate from it.

The analytical expression of the model with continuous variable (x,y) is (for the ease of presentation, we use the continuous variable),

$$m(x,y)= \sum_{i=1}^{i_1} z_i s_i = \sum_{i=1}^{i_1} [\sum_{j=1}^{j_i} z_{ij} + C_i] s_i \quad (1)$$

where C_i is the mean value of $\boldsymbol{R}_i$ and s_i (the i-th region function : functional form of $\boldsymbol{R}_i$)), z_{ij}

(the j-th sinusoid in $\boldsymbol{R}_i$), and z_i are respectively :

$$\begin{aligned} s_i &= 1, \in \boldsymbol{R}_i \\ &= 0, \textit{elsewhere.} \end{aligned} \tag{2}$$

$$\begin{aligned} z_{ij} &= A_{ij}\cos(\omega_{ij}^x x + \omega_{ij}^y y + \theta_{ij}) \\ &= \frac{A_{ij}}{2} e^{j(\omega_{ij}^x x + \omega_{ij}^y y + \theta_{ij})} + e^{-j(\omega_{ij}^x x + \omega_{ij}^y y + \theta_{ij})} \\ &= z_{ij}^+ + z_{ij}^- \end{aligned} \tag{3}$$

$$z_i = \sum_{j=1}^{j_i} z_{ij} + C_i \tag{4}$$

with $\omega_{ij}^x = 2\pi f_{ij}^x$, $\omega_{ij}^y = 2\pi f_{ij}^y$, which are the angular frequencies of the sinusoid for x and y axis respectively.

In the above expressions, for the simplicity of notation, we omitted the independent variables from $s_i(x,y)$, $z_i(x,y)$, $z_{ij}(x,y)$, $z_{ij}^+(x,y)$ and $z_{ij}^-(x,y)$. We will employ this notation henceforth.

Note that the index i refers to the texture region number and j refers to one of the sinusoids in that region.

In every mathematical development, we always respect the order (i.e., if A=B+C=D+E then B=D and C=E).

III. Frequency Domain Representation

In using (3), the expression in (1) can be rewritten as,

$$\begin{aligned} m(x,y) &= \sum_{i=1}^{i_1}\sum_{j=1}^{j_i} z_{ij}s_i + \sum_{i=1}^{i_1} C_i s_i \\ &= \sum_{i=1}^{i_1}\sum_{j=1}^{j_i} (z_{ij}^+ + z_{ij}^-)\, s_i + \sum_{i=1}^{i_1} C_i s_i \end{aligned} \tag{5}$$

Thus the frequency domain representation of multitexture image is :

$$\begin{aligned} M &= F[m] \\ &= F[\sum_{i=1}^{i_1}\sum_{j=1}^{j_i} (z_{ij}^+ + z_{ij}^-)s_i] + F[\sum_{i=1}^{i_1} C_i s_i] \\ &= \sum_{i=1}^{i_1}\sum_{j=1}^{j_i} (L_{ij}^+ + L_{ij}^-) + \sum_{i=1}^{i_1} L_i \end{aligned} \tag{6}$$

where F is the Fourier transform operator, $M = M(\omega_1, \omega_2)$, with spatial frequency (ω_1, ω_2), and $m = m(x,y)$. We will use these abbreviated notations henceforth. From (3) and (6), we see that

$$L_{ij}^+ = F[s_i z_{ij}^+] = \frac{A_{ij}}{2} e^{j\theta_{ij}} S_i^{+ij} \tag{7}$$

where

$$S_i^{+ij} = S_i(\omega_1 - \omega_{ij}^x, \omega_2 - \omega_{ij}^y) \tag{8}$$

with

$$S_i(\omega_1, \omega_2) = F[s_i]$$

We will use S_i in place of $S_i(\omega_1, \omega_2)$.

Thus the above expression becomes,

$$S_i = F[s_i] \tag{9}$$

Each S_i is centered at the zero frequency. $|S_i|$ has its maximum value at the zero frequency, and decreases as the frequency increases.

3.1 Positive Lump Element

In going from m to M, each sinusoid z_{ij} in $\boldsymbol{R}_i$ performs what follows and yields each L_{ij}^+ that we call positive lump element (PLE) : Modify S_i, which is the Fourier transform of the region function s_i to which it (the z_{ij}) belongs, with its characteristic parameters that we call CP's of z_{ij} which are $(\omega_{ij}^x, \omega_{ij}^y)$, θ_{ij}, and A_{ij}.

More specifically the modification performed by z_{ij} on S_i to give L_{ij}^+ is (see the final term in (7)) :

i) translation by $(\omega_{ij}^x, \omega_{ij}^y)$.

ii) phase rotation by θ_{ij}.

iii) multiplication by $\frac{A_{ij}}{2}$.

These PLE's are what we have to process to get each different region.

IV. Recovering a Texture Region

4.1 Amplitude Demodulation

By processing L_{ij}^+ as in (7), one can find out the i-th region function s_i.

Note that finding the region functions s_i for $1 \le i \le i1$ is finding all the texture regions and this is just what we want, the texture segmentation.

$$2|\ F^{-1}\ [L_{ij}^{+}]\ | = |\ F^{-1}[\ \frac{A_{ij}}{2} e^{\ j\theta_{ij}}\ S_i^{+\ ij}]|$$

$$= 2|\ \frac{A_{ij}}{2} e^{\ j(\theta_{ij} + \omega_{ij}^{x} x \omega_{ij}^{y} y)}\ s_i| = 2|\ s_i\ z_{ij}^{+}| = A_{ij}\ s_i \quad (10)$$

where F^{-1} is the inverse Fourier transform operator. Note that $|s_i| = s_i$ (because $s_i \ge 0$, $\forall(x,y)$: see (2)) is used in the above development.

The expression (10) means that by doubling the absolute value of the inverse Fourier transform of L_{ij}^{+}, one can obtain the i-th region function multiplied by the amplitude of the j-th sinusoid in that region.

Note that this j-th sinusoid is the very sinusoid which has modified the S_i with its CP's (see Section 3.1) to give the L_{ij}^{+}.

The relation (10) shows that among the three CP's of this sinusoid, only the amplitude A_{ij} affects the final result $A_{ij}\ s_i$ (neither the frequency nor the phase of the sinusoid).

The block diagram in Table 2 shows our entire process. We see the procedure of the relation (10) as a part of this procedure starting from L_{ij}^{+} to the end.

In this table, F and IFT are Fourier transform operator and Inverse Fourier transform operator respectively. $IFFR_{ij}^{+}$ is the Ideal Filter Frequency Response to be multiplied to M to extract only the L_{ij}^{+} in the frequency domain. This L_{ij}^{+} is inverse Fourier transformed to give $s_i\ z_{ij}^{+}$, and the absolute value of which will be doubled to get $A_{ij}\ s_i$. When this is obtained, the region $\boldsymbol{R}_i$ is obtained.

Table 2. Method for getting $A_{ij}\ s_i$ using ideal filter and amplitude demodulation.

표2. 이상적인 필터와 진폭복조를 이용하여 $A_{ij}\ s_i$ 를 얻는 방법

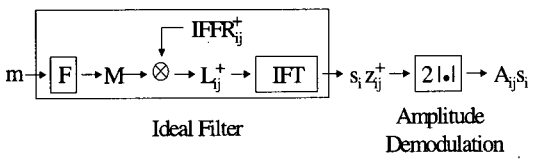

In fact, this is a kind of Amplitude Demodulation Method (called ADM henceforth), which consists of recovering the modulating signal s_i from the amplitude modulated signal $s_i\ z_{ij}^{+}$, where $z_{ij}^{+} = \frac{A_{ij}}{2} e^{\ j(\omega_{ij}^{x} x + \omega_{ij}^{y} y + \theta_{ij})}$ is a complex exponential carrier signal (see (3)).

Thus our system for the texture segmentation is very simple. It consists of two system components : the ideal filter to extract $s_i\ z_{ij}^{+}$ from the signal m, followed by the amplitude demodulation block which issues the double of the magnitude of its input.

Observe that there can be many ways to recover the region i : we can apply the method above to all the L_{ij}^{+}'s for j going from 1 to ji to find out the region i.

The only difference between all these regions found is their amplitude A_{ij}.

4.2 Gabor Filter

Thus far, it was implicitly supposed that exact L_{ij}^{+} can be extracted from M. We have seen that in this ideal case, we can recover exact texture regions (see (10)). But in reality, it is not possible because, as seen in (6), L_{ij}^{+}, for a given pair of i and j, is only one element of M where all the L_{ij}^{+}'s, all the L_{ij}^{-}'s, and all the L_i's are intermingled. Thus in practical cases, one is obliged to use a band pass filter to extract the desired L_{ij}^{+}. We use the 2-D Gabor filter for this because it has many desirable properties and especially it gives optimum space bandwidth product[1].

The use of Gabor filter will result in approximate L_{ij}^{+} denoted by $\tilde{L}_{ij}^{+}$ (approximate APLE (Approximate PLE) henceforth) and the subsequent amplitude demodulation also results in approximate s_i

Table 3. Method for getting $A_{ij}\tilde{s}_i$ using Gabor filter and amplitude demodulation.

표3. 게이버 필터와 진폭복조를 이용하여 $A_{ij}\tilde{s}_i$ 를 얻는 방법

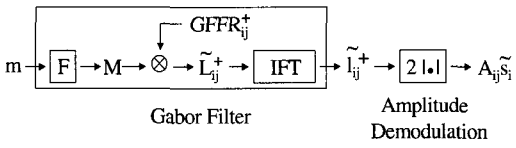

denoted by $\tilde{s}_i$.

In Table 3, we show the modified method of that shown in Table 2, where the Gabor filter replaces the ideal filter.

In this table,

$$T_{ij}^{+} \doteqdot \tilde{s}_i \, z_{ij}^{+} \tag{11}$$

and $GFFR_{ij}^{+}$ is the Gabor Filter Frequency Response centered at $(\omega_{ij}^{x}, \omega_{ij}^{y})$ to extract T_{ij}^{+}. This T_{ij}^{+} is inverse Fourier transformed to give T_{ij}^{+} (see (11)), which will be amplitude demodulated to get $A_{ij}\tilde{s}_i$. When this is obtained, the region $\boldsymbol{R}_i$ is obtained approximately.

The only difference between Table 2 and Table 3 is that the ideal filter is replaced by the Gabor filter in practical case and this results in recovering the texture regions approximately.

The analytical expression in spatial domain of the Gabor filter used in this paper is (there are many articles where the analytical expression of Gabor filters are shown[2]-[5]),

$$h(x,y) = g(x,y)\, e^{-j2\pi(\omega^x x + \omega^y y)} \tag{12}$$

where the Gaussian function $g(x,y)$ is given by,

$$g(x,y) = \frac{1}{2\pi\sigma^2} e^{\frac{-(x^2+y^2)}{2\sigma^2}} \tag{13}$$

Thus $h(x,y)$ is a complex sinusoid modulated by a 2-D Gaussian function.

The 2-D Fourier transform of $h(x,y)$, which is the frequency response of the Gabor filter, denoted by $H(\omega_1, \omega_2)$ is given by,

$$H(\omega_1, \omega_2) = e^{-2\pi^2\sigma^2[(\omega_1-\omega^x)^2+(\omega_2-\omega^y)^2]} \tag{14}$$

We see that this is a circularly symmetric Gaussian function centered at (ω^x, ω^y) with σ determining the bandwidth. We used this filter to extract the desired L_{ij}^{+} in adjusting the (ω^x, ω^y) and σ.

Note that,

$$GFFR_{ij}^{+} = H(\omega_1, \omega_2) \tag{15}$$

with $(\omega^x, \omega^y) = (\omega_{ij}^{x}, \omega_{ij}^{y})$ in (14).

Till now, we have examined the theoretical framework for the segmentation of 2-D multitexture image.

In the next Sections, we present the experimental results obtained in applying the theoretical results.

V. Data Description

5.1 Input data Description

We use a synthetic multitexture image of size 256x256 with 3 texture regions : $\boldsymbol{R}_1$, $\boldsymbol{R}_2$, and $\boldsymbol{R}_3$. Every texture region contains a mean value and sinusoids with discrete independent variables (x,y). The next is the analytical description of each region.

$Z=AB+C$, where $Z = [z_1\ z_2\ z_3]^T$

(see (4) for z_1, z_2 and z_3),

$A = [a_{ij}]$ with $a_{ij} = A_{ij}$,

$B = [b_{ij}]$ with $b_{ij} = \cos(\omega_{ji}^{x}x + \omega_{ji}^{y}y)$, and

$C = [C_1\ C_2\ C_3]^T$.

Note that the image m will have the next expression :

$m = [s_1\ s_2\ s_3]\ Z$ (see (1))

Note also that we have omitted the phase from every sinusoid because we found that it did not influence the segmentation result : see b_{ij} above.

The indices i and j of a_{ij} and b_{ij} are respectively the row and column numbers of the matrix elements. Also the T for the vectors means the transpose. The numerical values of A and C are :

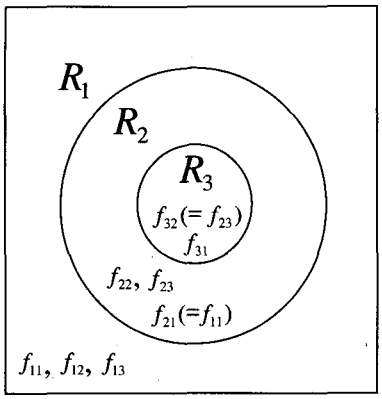

Fig. 1. Distribution of the texture regions.
그림 1. 각 텍스쳐 영역의 배치상황

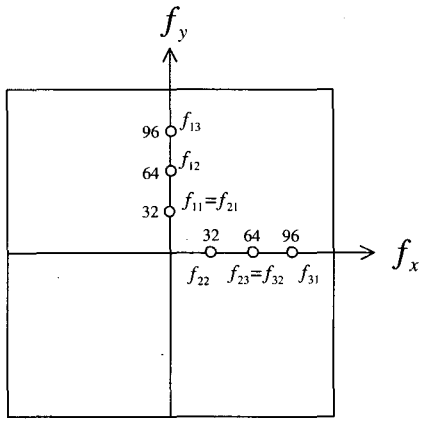

Fig. 2. Position in the frequency domain of each sinusoid in the synthetic texture image.
그림 2. 합성한 텍스쳐영상에 존재하는 각 정현파의 주파수 영역에서의 위치

$$A=\begin{bmatrix}5&3&8\\10&2&3\\7&6&0\end{bmatrix},\quad C=[3\ 5\ 8]^T \tag{16}$$

For B, all the ω_{ij}^x's and ω_{ij}^y's are,

$$\begin{bmatrix}\omega_{11}^x&\omega_{12}^x&\omega_{13}^x\\\omega_{21}^x&\omega_{22}^x&\omega_{23}^x\\\omega_{31}^x&\omega_{32}^x&\omega_{33}^x\end{bmatrix}=(2\pi/256)\begin{bmatrix}0&0&0\\0&32&64\\96&64&0\end{bmatrix}$$

and

$$\begin{bmatrix}\omega_{11}^y&\omega_{12}^y&\omega_{13}^y\\\omega_{21}^y&\omega_{22}^y&\omega_{23}^y\\\omega_{31}^y&\omega_{32}^y&\omega_{33}^y\end{bmatrix}=(2\pi/256)\begin{bmatrix}32&64&96\\32&0&0\\0&0&0\end{bmatrix}$$

The position of each texture region is given in Fig 1, where fij = (f_{ij}^x, f_{ij}^y) =($256\omega_{ij}^x/2\pi$, $256\omega_{ij}^y/2\pi$) is the frequency of the j-th sinusoid in R_i.

And the position of each sinusoid in the frequency domain is in Fig. 2.

With this synthetic multitexture image, we performed 4 experiments, throughout which we verified if our method works for a synthetic multitexture image, and tried to see what kind of situations will occur depending on the selection of Γ_{ij}^+ in the frequency domain.

The selection is done by multiplying M with $GFFR_{ij}^+$ tuned to $(\omega_{ij}^x, \omega_{ij}^y)$ (see Table 3 and (15)).

Once Γ_{ij}^+ is selected and extracted by the above multiplication, we proceed with the inverse Fourier transform and amplitude demodulation to find out the approximate i-th region function $\tilde{s}_i$.

5.2 Resulting Figures Description

In the following, we will show the results of 4 experiments with 4 figures. Every figure is composed of four sub-figures and for each figure (in the next, we will refer to Fig. 3 for the presentation of each sub figure but the same is true for the other figures, too),

(a) : Synthetic multitexture image we used.

(b) : Amplitude spectrum of the image in (a) with the Gabor filter frequency response, tuned to fij (see Fig. 1), juxtaposed (both are in log-magnitude plot and they are presented in such a way that the brighter the point is, the higher the peak at that location is). Note the high values at the locations corresponding to the frequencies marked in Fig. 2 and at the symmetrically opposed locations relative to the origin (due to the fact that the image is real valued). We marked the position of the center frequencies fij to which the Gabor filter is tuned, by the brightest point. The bandwidth of the Gabor filter is adjusted by choosing σ manually in such a way that it filters only the frequency region

around the desired fij.

(c) : Recovered region. This shows $A_{ij}\tilde{s}_i$, where the sinusoid with selected fij exists. Note that the procedure (10) finds out all the regions where the sinusoid with frequency fij exists (see Fig. 4 for example. This will be verified in Section 6.2).

(d) : Strictly speaking, this is not the carrier signal. It is $\tilde{s}_i z_{ij}$. One can see the sinusoid with frequency fij (i.e., z_{ij}) in $\tilde{s}_i$.

VI. Experimental Results

Throughout all the four experiments, we could verify the theoretical results. We will present them in ascending order of number of chosen APLE's.

6.1 Only one region is detected with only one APLE

Fig. 3(c) is obtained by filtering the image with a Gabor filter tuned to f22 (the brightest point on (b) of the figure ; also see Fig. 2.) to extract L_{22}^{+} and by processing the latter with ADM. This sub-figure shows what the theoretical analysis predicts : approximate region function $\tilde{s}_2$ multiplied by the amplitude of the second sinusoid ($A_{22}=2$: see (16)) in the region $\boldsymbol{R}_2$ to the frequency of which the Gabor filter is tuned.

We have made other similar experiments by tuning the Gabor filter to the frequencies f12, f13, and f31 (note that each of these four frequencies, including f22, exists only in one region : see Fig. 1) and we recovered $\boldsymbol{R}_1$, $\boldsymbol{R}_1$, and $\boldsymbol{R}_3$ respectively. All the results coincided with the theoretical results.

6.2 Two regions are detected with only one APLE

Fig. 4(c) shows the result of tuning the Gabor filter

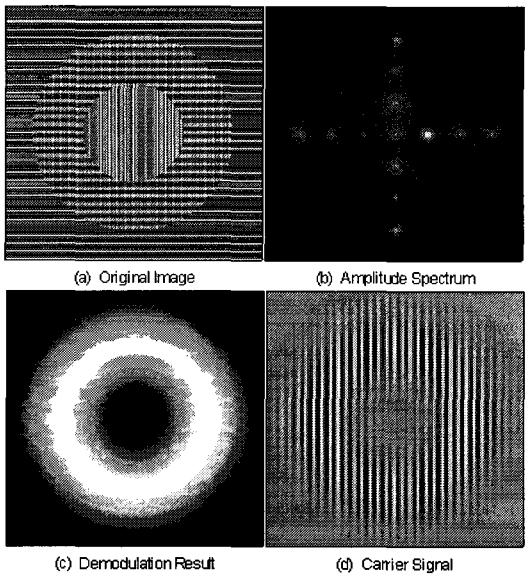

Fig. 3. L_{22}^{+} corresponding to f22 is extracted by $GFFR_{22}^{+}$ and ADM is applied. On (c), only $\boldsymbol{R}_2$ is detected.

그림 3. $GFFR_{22}^{+}$ 로 f22 에 대응되는 L_{22}^{+} 를 추출한 후 ADM을 적용. (c) 에 검출된 $\boldsymbol{R}_2$ 만이 보인다.

to another frequency f23 existing in $\boldsymbol{R}_2$ and $\boldsymbol{R}_3$, which are the detected regions.

It is not surprising to see multiple regions detected in processing only one APLE : L_{23}^{+} in this case.

We will demonstrate this using the ideal case. L_{23}^{+} and L_{32}^{+} are centered at the same frequency in the frequency domain because f23 = f32 (see Fig. 2). Thus when L_{23}^{+} is chosen to be processed for the demodulation, L_{32}^{+} is also chosen (we suppose that the gabor filter frequency response covers the two PLE's) and when the ADM is applied, it is applied to the sum of L_{23}^{+} and L_{32}^{+} as follows (see (10)) :

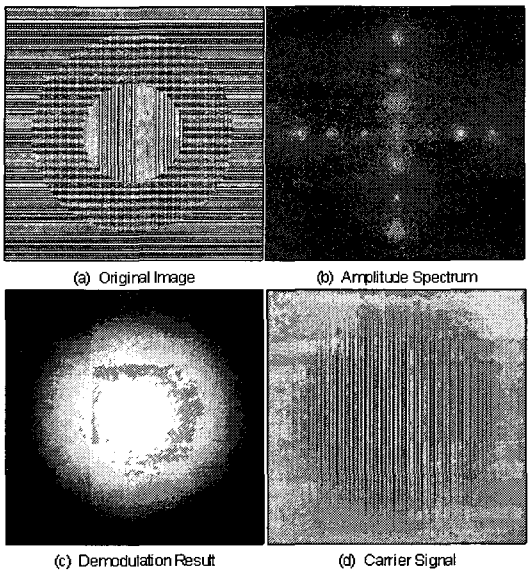

Fig. 4. L_{23}^{+} corresponding to f23 is extracted by $GFFR_{23}^{+}$ and ADM is applied. On (c), R_2 and R_3 are detected.

그림 4. $GFFR_{23}^{+}$ 로 f23 에 대응되는 L_{23}^{+} 를 추출한 후 ADM을 적용. (c) 에 검출된 R_2 와 R_3 가 보인다.

$$
\begin{aligned}
& 2| F^{-1}[L_{23}^{+}+L_{32}^{+}] | \\
& = 2| F^{-1}[\frac{A_{23}}{2} e^{j\theta_{23}} S_2^{+23}+\frac{A_{32}}{2} e^{j\theta_{32}} S_3^{+32}]| \\
& = | e^{j\omega_{23}^{x}x} e^{j\omega_{23}^{y}y}[A_{23}e^{j\theta_{23}} s_2+A_{32}e^{j\theta_{32}} s_3] | \\
& = | A_{23}e^{j\theta_{23}} s_2 A_{32}e^{j\theta_{32}} s_3 | \\
& = | A_{23}e^{j\theta_{23}} s_2 |+| A_{32}e^{j\theta_{32}} s_3 | \\
& = A_{23} s_2+A_{32} s_3
\end{aligned}
\qquad (17)
$$

where, $(\omega_{23}^{x}, \omega_{23}^{y}) = (\omega_{32}^{x}, \omega_{32}^{y})$ and the fact that s_2 and s_3 are mutually exclusive (i.e., when s_2=1, s_3=0, and when s_3=1, s_2=0) is used for the development.

The final expression in (17) says that the two region functions s_2 and s_3 will be recovered with their height multiplied by respective amplitude of the sinusoid with frequency f23 in each own region.

This result is shown in Fig. 4(c) : the detected two regions are of different grey levels (R_3 is brighter than R_2).

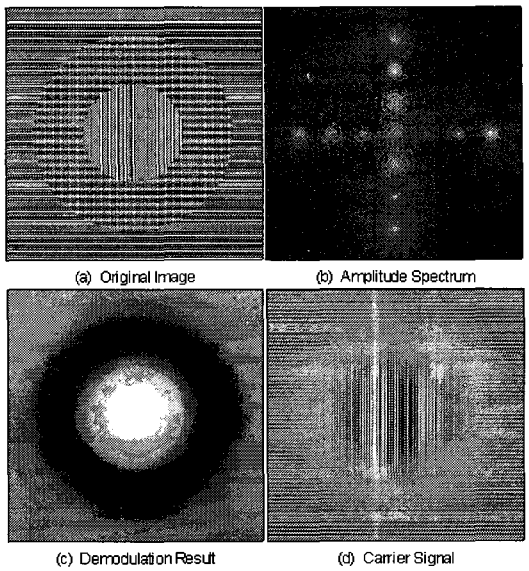

Fig. 5. L_{12}^{+} and L_{31}^{+} corresponding to f12 and f31 are extracted by $GFFR_{12}^{+}$ and $GFFR_{31}^{+}$ respectively and ADM is applied. On (c), R_1 and R_3 are detected.

그림 5. $GFFR_{12}^{+}$ 와 $GFFR_{31}^{+}$ 로 f12 와 f31 의 각각에 대응하는 L_{12}^{+} 와 L_{31}^{+} 를 추출한 후 ADM을 적용. (c) 에 검출된 R_1 과 R_3 가 보인다.

This is due to the fact that the amplitude of the sinusoid with frequency f23 in R_2 is smaller than that of the sinusoid with frequency f32 (=f23) in R_3. Effectively, A_{23}=3 and A_{32} = 6.

This experiment shows that it is possible to identify multiple texture regions by extracting and amplitude demodulating only one PLE. This is always possible whenever a sinusoid of same frequency exists in multiple texture regions.

6.3 Two regions are detected with two APLE's

Fig. 5(c) shows the result of using two Gabor filters : one is tuned to f12 and the other to f31. Each of these two frequencies exists in only one region and they are not in the same region.

Each Gabor filter finds different region.

The difference of grey levels between the two regions comes from the difference of the amplitudes $A_{12}=3$ and $A_{31}=7$. Note the proportionality of the grey levels of the regions : A_{12} / A_{31} = (brightness of $\boldsymbol{R}_1$) / (brightness of $\boldsymbol{R}_3$). $\boldsymbol{R}_2$ is not detected (completely dark) because there is neither f12 nor f31 in it.

Every region where there is not the sinusoid to the frequency to which the Gabor filter is tuned will always appear completely dark.

6.4 Three regions are detected with three APLE's

In this Section, three Gabor filters are used to be tuned to three different frequencies. Each of these frequencies exists in only one region and they are not in the same region.

This results in detection of three different regions as seen in Fig. 6(c). The difference of grey levels between the three regions comes from the difference of the amplitudes $A_{12}=3$, $A_{22}=2$, and $A_{31}=7$. As in the previous experiment, the grey level of each region is proportional to these values.

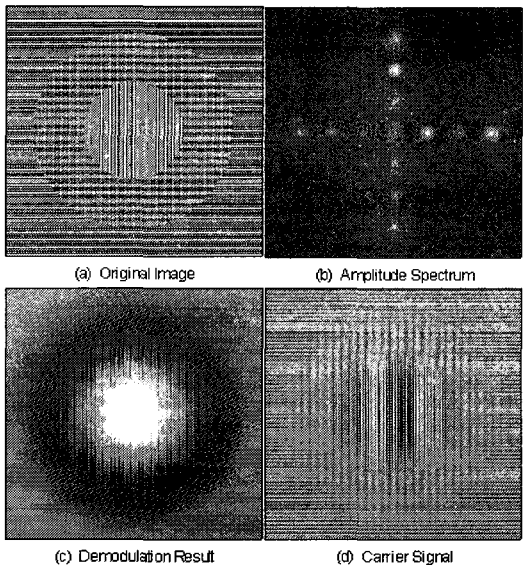

Fig. 6. Γ_{12}^{+}, Γ_{22}^{+}, Γ_{31}^{+} corresponding to f12, f22, and f31 are extracted by $GFFR_{12}^{+}$, $GFFR_{22}^{+}$, and $GFFR_{31}^{+}$ respectively and ADM is applied. On (c), $\boldsymbol{R}_1$, $\boldsymbol{R}_2$, and $\boldsymbol{R}_3$ are detected.

그림 6. $GFFR_{12}^{+}$ 와 $GFFR_{22}^{+}$ 그리고 $GFFR_{31}^{+}$ 로 f12, f22 와 f31 의 각각에 대응하는 Γ_{12}^{+}, Γ_{22}^{+} 와 Γ_{31}^{+} 를 추출한 후 ADM을 적용. (c) 에 검출된 $\boldsymbol{R}_1$, $\boldsymbol{R}_2$ 그리고 $\boldsymbol{R}_3$ 가 보인다.

VII. Discussion

In Section VI, we presented four experimental results obtained by applying our method of segmentation to a synthetic multitexture image.

All the results followed very faithfully what was anticipated by the theoretical results.

We found that our method, with the aid of amplitude demodulation after the Gabor filtering, recovers all the texture regions containing the sinusoid with frequency to which the Gabor filter is tuned.

If every texture region is distinguished by its dominant spatial frequency as is our assumption, our method will work well even when the image is a natural multitexture image (in case when the assumption is not respected (random textures), we incorporate a Gaussian lowpass filter after the amplitude demodulator : this case is under investigation and we find that deciding suitable tuning frequency and bandwidth of the Gabor filter and the Gaussian lowpass filter is very important).

The experimental results prove that our method is based on a solid foundation. The method we have proposed has to be armed with an algorithm for deciding the parameters of the Gabor filter (i.e., the

tuning frequency and the bandwidth) automatically.

Future research has to be focused on the design of the Gabor filters and the Gaussian lowpass filters to be used for the natural multitexture image segmentation. We use a multichannel structure with each channel containing a Gabor filter, an Amplitude Demodulator and a Gaussian filter in our ongoing research for the natural multitexture image segmentation.

VIII. Conclusion

In this paper, we assume that every texture is distinguishable because each texture has its own dominant spatial frequencies different from those of the other textures.

And also we conjecture that multitexture image is an ensemble of non overlapping adjacent region functions, each of which has value 1 in its own region and 0 elsewhere, and that each of these region functions is multiplied by the sum of many sinusoids and the mean value in its own region.

This conjecture has led us to the texture segmentation algorithm consisting of Gabor filtering followed by the Amplitude Demodulation.

We found that our method recovers all the texture regions containing the sinusoid with frequency to which the Gabor filter is tuned. We have demonstrated the discriminating power of our method in using a synthetic multitexture image. The experimental results prove that our method is based on a solid foundation.

Our method is very simple and also very efficient. It permits us to avoid many of the problems encountered in classifying the feature vectors calculated in sliding a window on the texture image in case of widely used feature-based approach for the texture segmentation.

References

[1] R.N.Barcewell. The Fourier Transform and its Applications, New York, McGraw-Hill, 1978.

[2] R.Mehrotra, K.R.Namuduri, and N. Ranganathan "Gabor Filter-Based Edge Detection" Pattern Recognition, vol.25, No.12, pp. 1479-1494, 1992.

[3] M.R.Turner "Texture Discrimination by Gabor Functions" Biological Cybernetics 55, pp. 71-82, 1986.

[4] Andreas Teuner, Olaf Pichler, and Bedrich J. Hosticka "Unsupervised Texture Segmentation of Images Using Tuned Matched Gabor Filters" IEEE Trans. on Image Processing, Vol. 4, No. 6, pp. 863-870, June 1995.

[5] Dannis Dunn and William E. Higgins "Optimal Gabor Filters for Texture Segmentation" IEEE Trans. on Image Processing, Vol. 4, No. 7, pp. 947-964, July 1995.

[6] Todd R.Reed and J.M.Hans du Buf "A Review of Recent Texture Segmentation and Feature Extraction Techniques" CVGIP : Image Understanding Vol.57, No.3, pp.359-372, May 1993.

저 자 소 개

李 賢 秀

1974 년 2 월 : 서울대학교 전자공학과 졸업 (공학사)
1982 년 9 월 : 베장송대학 컴퓨터 공학과 졸업 (공학석사)
1992 년 4 월 : 르 아브르대학 졸업 : Image Processing 전공 (공학박사)
1993 ~ 현재 : 명지대학교 정보통신공학과 교수
관심분야 :텍스쳐 분석 및 합성, 패턴 인식, 3 차원 모델기반 이동물체 추적, 지문인식